Binding of an Antifreeze Polypeptide to an Ice/Water Interface via Computer Simulation

Shawn M. McDonald, Angela White, and Paulette Clancy
School of Chemical Engineering, Cornell University, Ithaca, NY 14853

John W. Brady
Dept. of Food Science, Cornell University, Ithaca, NY 14853

The interaction between a winter flounder antifreeze polypeptide and an ice/water interface was studied using Molecular Dynamics computer simulation techniques to study the mechanism of action of this class of antifreeze molecules. Simple Point Charge models were used for the water molecules, and a molecular mechanics program (CHARMM) was used to construct the model for the polypeptide. A $(20\bar{2}1)$ face was exposed on the ice surface, as this is believed to be the experimentally favored ice face for peptide binding. The polypeptide binds strongly to the ice surface even though it was placed with its four polar threonine (Thr) groups pointing away from the ice surface. This tested the previously advanced hypothesis that adsorption occurs primarily between these groups and the ice due to a matching of the spacing between oxygen atoms in the ice lattice and the polar Thr residues. As well as contacts with other polar groups on the peptide, the binding to the ice produces a good steric fit of the peptide with the corrugated ice interface. The presence of the peptide did not induce any melting of the ice at 200 K.

Introduction

Antifreeze polypeptides are a class of molecules capable of acting as cryoprotectants, allowing, for example, antarctic fishes to live in temperatures below 0°C. These polypeptides are believed to act by adsorption to a planar ice front through hydrogen-bonding to the oxygen atoms in the ice lattice (Knight et al., 1991; Chakrabartty et al., 1989b). Most cryobiologists assume that this binding occurs between polar groups on the peptide (attention has focused almost entirely on the four threonine residues that the molecule possesses) and water molecules on the surface of the ice lattice. In this article we examine the binding of a winter flounder antifreeze polypeptide, HPLC-6, to an ice/water interface using molecular dynamics (MD) simulation methods to explore the validity of this hypothesis.

The winter flounder peptide chosen here contains 37 amino acid residues whose sequence is $Asp-Thr-Ala-Ser-Asp-(Ala)_6-Leu-Thr-Ala-Ala-Asn-Ala-Lys-(Ala)_3-Glu-Leu-Thr-Ala-Ala-Asn-(Ala)_7-Thr-Ala-Arg$ (Fourney et al., 1984). Thus it contains three repeating segments of the type $Thr-(Xaa)_2-Asx-(Xaa)_7$, where *Xaa* is mainly alanine. Similar alanine-rich repeating segments, 11 amino acids in length, have been discovered for antifreeze proteins from yellowtail flounder (Scott et al., 1987) and from the sculpin family (Hew and Fletcher, 1985; Feeney et al., 1986; Davies et al., 1982; Pickett et al., 1984). The winter flounder antifreeze polypeptide (AFP) HPLC-6 has been shown, by circular dichroism spectroscopy and X-ray crystallography, to exist in a mainly α-helical conformation in solution near 0°C, with a melting temperature near 18°C (Chakrabartty et al., 1989a; Yang et al., 1988). A helical structure does not imply antifreeze activity, however, since the fragment GluLeu12–Arg37 has a largely helical conformation but lacked antifreeze activity.

The winter flounder AFP molecule contains several polar threonine residues whose side chains align along one side of the helix. These side chains have received most of the attention of the experimental community who have assumed that, since the spacings between the Thr groups in this peptide match those of an idealized ice lattice, the Thr groups will form the primary contacts to the ice (Knight et al., 1991;

Correspondence concerning this article should be addressed to P. Clancy.

Eastman and DeVries, 1980; Chou, 1992), thereby retarding further ice crystal growth. It is indeed likely that the adsorption of molecules on solid surfaces will depend critically on the exact chemical nature of the contact groups and their relative positions along the peptide chain. This has been confirmed by experimental studies of the adsorption of fibronectin and glucagon to bare surfaces of metals (Grinnell and Feld, 1982; Pitt et al., 1986) and plastics (Horbett, 1981; Lu and Park, 1991). However, there are as yet no experimental studies that provide the molecular-level detail necessary to determine the contact groups for the binding of antifreeze polypeptides to ice interfaces.

There is considerable commercial interest in understanding the mode of activity of these molecules. They are currently used industrially to preserve bovine and other embryos, they are under investigation to help prevent natural gas hydrate formation in pipelines, and a clone is used to preserve the flavor of foods such as ice cream. Other applications in biomedical, aviation, and agricultural applications are possible, though their implementation is likely to be hastened if mechanistic information about the wild-type could be used to "engineer" mutated polypeptides with enhanced ability.

MD simulation techniques offer a way to provide this information in principle, though there are a number of practical difficulties due to the prohibitively large computational effort involved in simulating the detailed intermolecular forces between every atom in the relatively large systems needed to contain the AFP and surrounding ice and water molecules (of the order of thousands of water molecules). Other difficulties involve the short timescales that can be monitored (of the order of ns) and the sluggish kinetics of ice-containing systems at temperatures around the melting point. Despite these difficulties, there is considerable incentive to use MD simulation techniques for this problem, as they represent a completely noninvasive *in situ* tool. These techniques are capable of providing exquisitely detailed information about the groups involved in binding the peptide to the ice interface in a manner unlikely to be duplicated by experimental studies.

In the past, there has been very little simulation work devoted to the adhesion of biomolecules to solid surfaces. There are, however, two recent articles that describe the binding of the winter flounder antifreeze polypeptide (HPLC-6) to a bare (simply terminated) ice surface with a $(20\bar{2}1)$ exposed face, that is, this is a simplification of the real situation since the surrounding liquid water molecules are absent. Lal et al. (1993) described this "docking" through energy minimizations using the COMMET software molecular mechanics package (White and Morrow, 1979) to define the optimum angular positioning of the peptide on the surface. The peptide preferred to lie at an angle of about 60° across the ridges in the corrugated $(20\bar{2}1)$ face. Later Madura et al. (1994) performed a simulation of the D- and L-forms of the HPLC-6 AFP, also at a bare $(20\bar{2}1)$ ice surface using CHARMM 22 to model the AFP and TIP3 to model the water. They reproduced the experimental findings that the two isomers should bind to the ice in mirror symmetry-related directions.

Our docking studies using the CHARMM22 program to investigate the energy of the interaction of the peptide with a bare ice surface for over 40 different rotations and translations of the peptide at the ice surface essentially duplicated Lal's result that the peptide preferred to lie across the ridges in the ice surface when the peptide was bent at 30° and 60°, but not for a straight peptide. Earlier hydration studies of ours had shown the peptide to prefer to adopt a bent conformation in solution, a roughly 30° bend at 300 K and a 60° bend at 273 K (McDonald et al., 1993).

Our main goal here was to perform the first reported MD simulation of the binding of a wild-type peptide at the full ice/water interface, not the ice/vacuum interface studied by all previous investigators. This describes the environment experienced by the real molecule *in situ* far more realistically than the artificial environment in the "docking" studies. On a practical note, comparison of the results found here with docking studies should allow us to determine whether the results are sufficiently different to warrant the large computational burden imposed by the full ice/water + peptide simulation. As a rough guide, a comprehensive docking study would take 1–2 days of elapsed time, whereas 100 ps of MD simulation for a large ice/water + peptide system would take a month on a fast workstation (such as an IBM RS6000-500). The MD results are arguably the only way to provide insight into the mechanism of action of the winter flounder antifreeze polypeptide.

As well as calculating the binding of the peptide to the ice, a secondary goal was to study the effect of the peptide on the ice front. For instance, would the presence of the peptide cause the ice to melt? The ice is highly unlikely to grow during the MD simulation due to its sluggish kinetics at the temperature considered here (200 K), the ice point for this water model (Karim et al., 1990). It is important to realize that the numerical value of the melting point of the model (200 K for the simple point charge (SPC) model for water vs. 273 K for real water) is unimportant for determining the properties of the system as long as the reduced temperature (T/T_m) at which the study is carried out corresponds to an appropriate location on the phase diagram of the model. As such, our simulation is being performed in the operating regime of natural antifreeze molecules, that is, around the ice point. This simulation may also provide us with information regarding any changes in the structure of the AFP molecule induced by the ice. This structure can be studied in terms of its conformation and helix-stabilizing interactions in comparison to its behavior in pure water, which we studied earlier (McDonald et al., 1993).

Simulation Methodology and Potentials Used

Intermolecular potentials

The modeling of the interactions between water molecules was achieved using the rigid three-site SPC (Single Point Charge) model due to Berendsen et al. (1981). The potential energy function, E_p, of the SPC model includes both van der Waals and electrostatic terms and has the form:

$$E_p = \sum k_b (b - b_0)^2 + \sum k_\theta (\theta - \theta_0)^2 + \sum_{ij} 4\epsilon_{ij}\left[\left(\frac{\sigma_{ij}}{r_{ij}}\right)^{12} - \left(\frac{\sigma_{ij}}{r_{ij}}\right)^{6}\right] + \sum_{ij} \frac{q_i q_j}{4\pi\epsilon_0 r_{ij}}. \quad (1)$$

The values of the equilibrium bond length, b_0, and the equi-

librium bond angle (H–O–H), θ_0, are 1.00 Å and 109.47° for the SPC model. Interactions of the van der Waals type (12–6) are only allowed between oxygen atoms.

The O–H distances are constrained using the iterative SHAKE algorithm (Van Gunsteren and Berendsen, 1977). Partial charges are centered on each site. This model provides a good description of the liquid properties, especially diffusion coefficients, as compared to experiment.

The polypeptide was modeled using the molecular mechanics software package CHARMM22 (Brooks et al., 1983) using an intermolecular potential of the form:

$$E_p = E_b + E_\theta + E_\phi + E_\omega + E_{vdw} + E_{el} + E_{hb} + E_{cr} + E_{c\phi}. \quad (2)$$

This function includes a set of terms to account for internal motions within the molecule and another set of terms that model three types of nonbonded interactions within a molecule or between molecules. Nonbonded interactions within the CHARMM force field involve van der Waals terms E_{vdw}, electrostatic terms E_{el}, hydrogen bonding contributions (E_{hb}), and two constraint terms, E_{cr} and $E_{c\phi}$. There are a number of methods for handling the van der Waals and electrostatic terms within CHARMM. One can use a switching function applied over a small window of separation distances to smooth the nonbonded interactions to zero at a certain cutoff distance. Alternatively, a shifting function can be applied to the nonbonded interactions for all separation distances up to a set cutoff value. Most of the atoms in a given system have an assigned van der Waals radius, σ, and well depth, ϵ, that describes the strength of the van der Waals interaction. The electrostatic interactions were cut off at a distance of 10 Å using a shifting function on an atom-pair basis. The nonbond list was cut off at a separation of 12 Å on an atom-pair basis and was updated every 10 timesteps. The van der Waals interactions were cut off at a distance of 10 Å using the atom-pair shifting function.

A detailed description of this model for the peptide and its behavior *in vacuo* and in water have been given previously (McDonald et al., 1993). Periodic boundary conditions were used in the plane of the ice surface (that is, x- and y-), a fixed lattice was used at the base of the ice block, and a free surface existed above the water region (that is, there was no periodic boundary in the z-direction). The simulation was conducted at a constant temperature of 200 K (the ice point of the model), that is, under NVT ensemble conditions, where there is a constant number of particles, N, constant volume, V, and constant temperature, T. No pressure bath was used. The reduced density of the liquid water was 0.9 g/cm^3.

Initial conformation of the peptide

The equilibrated conformation of the polypeptide resulting from a 1.8-ns (1,800,000 time step) MD simulation *in vacuo* at 300 K was used as the starting point for an energy minimization of the peptide "docked" with a bare ice surface exposing a (20$\bar{2}$1) orientation. The *in vacuo* simulation resulted in a peptide bent to about 60° about the intact salt bridge formed in the middle of the peptide between Lys 18 and Glu 22. Energy minimization, consisting of 10 steps of steepest descent and up to 2,500 steps of an adopted basis Newton-Raphson method, resulted in a conformation in which the salt bridge lay at an angle of 160° away from the ice and the threonine groups were also pointing away from the ice. However, there was a good fitting of the shape of the peptide in the "hills and valleys" of the molecularly rough (20$\bar{2}$1) interface. Energy minimizations of 45 different rotational and translational arrangements of the peptide at the ice surface were conducted to ensure that the lowest energy configuration was achieved and local minima avoided. The lowest energy arrangement of the peptide was used to set up the MD simulation as described below. Repeating the study with an *unbent* polypeptide, identical to the first system except for the bend, showed little difference in the lowest energy configuration. However, it did alter the groups within contact range of the ice: the unbent peptide had the four Thr groups close to the ice, although only one of these groups formed a hydrogen bond with the ice, and the bent one had two Thr groups (Thr 13 and 24) and one Asn group (Asn 16) in contact with the solid, with only the Asn side chain forming hydrogen bonds to the ice. Lacking experimental data, we cannot yet say whether the real AFP is bent in solution or in contact with ice.

We chose to consider the behavior of the bent peptide at an ice/water interface for two reasons: first, all the simulations we have performed for the wild-type winter flounder polypeptide have exhibited a bend whether *in vacuo* or in solution at both 200 and 300 K. All the tests performed so far do not indicate this bend to be a peculiarity of the parameters chosen for the peptide or the water model. There are helices in globular proteins, such as retinol binding protein (Aqvist et al., 1986) or calmodulin (Barbato et al., 1992; Rao et al., 1992), that have been seen to be bent in experimental studies. Second, since a bent peptide shows a preferred orientation with the Thr groups pointing out into the liquid side of the interface, unlike the model suggested by Knight et al. (1991) in which the threonines were the main contacts to the ice, we can test whether the hydrogen bonding of Thr groups to the ice is indeed the primary binding mechanism. If steric fit is important, as the "docking" results of Lal et al. (1993), Madura et al. (1994), and ourselves (McDonald et al., 1994) have demonstrated, then intentionally placing the peptide with the Thr groups away from the ice could help evaluate the importance of Thr group binding relative to the advantages due to steric fitting of the peptide shape with the interface.

Assembly of the ice/water/peptide system

The first step in the simulation of the wild-type polypeptide near an ice/water interface involved construction and equilibration of the ice/water interface without the AFP molecule present. The ice was chosen to have a (20$\bar{2}$1) crystallographic orientation since this was the plane to which adsorption of the wild-type AFP had occurred in etching experiments (Knight et al., 1991). Simulations of bulk phases of ice exist (Han and Hale, 1992; Deutsch et al., 1983b; Weber and Stillinger, 1983); we note in particular, the work of Hale et al. simulating bulk ice I_h using the Monte Carlo method (Ward et al., 1982). The optimum parameter set for water molecules in the hexagonal ice lattice found by Hale et al. (Deutsch et

al., 1983a) involved an H–O–H bond angle of 101° and an O–H bond length of 0.97 Å, subsequentially different from the values of the SPC model used here (109.47° for the bond angle and 1.00 Å for the O–H bond length). This difference is not surprising since the SPC model was fitted to liquid phase properties at room temperature only.

A large block of ice was fabricated by duplicating in space a small rectangular region of ice I_h. This region of ice was created by placing oxygen atoms of water molecules on lattice positions provided by Hale (Deutsch et al., 1983b) and the coordinates of the hydrogen atoms were made to fit the geometry of the SPC water model starting from those given in the coordinate set by Hale. The large block of ice was cut with two parallel planes to expose the $(20\bar{2}1)$ AFP adsorption plane. The slab was rotated such that its smallest dimension was set perpendicular to the z-direction. At this point, the slab contained four molecular layers of width 3.5 Å each in the z-direction. The coordinates of this solid region were duplicated twice in the $+z$-direction to provide the coordinates for what would become the liquid region and once in the $-z$-direction to create the eight-layer-wide solid region. A copy of a four-layer-wide slab was added to these two blocks of ice to act as a fixed lattice in the subsequent simulations.

The ice/water interface was equilibrated using two segments of MD. First, the last eight layers of the large ice slab were heated to 275 K and then equilibrated for 12 ps to produce a liquid phase, as described for the MD simulations of the wild-type AFP in water (McDonald et al., 1993). The positions of the atoms in the solid and in the fixed lattice were held fixed during the heating. The liquid was then cooled to 200 K (using velocity scaling) and equilibrated further for 6 ps. Then the constraints on the water molecules in the solid region were released and the system was equilibrated for 10 ps at 200 K. This resulted in an overall ice/water system with dimensions 85 Å by 37 Å by 52 Å, incorporating 4,856 molecules of water in total, of which 2,507 were initially located on ice lattice sites.

The location of the ice/water interface was determined using a combination of analysis techniques: the properties of "slices" of the system, cut to encompass one plane of molecules in the ice lattice and continued into the liquid without changing the thickness of the slice, were evaluated for their diffusion coefficient and density. In previous studies of metals, semiconductors, Lennard-Jones systems, and natural gas hydrates, this technique was found to be accurate and efficient (Cook and Clancy, 1993).

Once the ice/water system had been equilibrated, a single wild-type AFP molecule was inserted into the ice/water interfacial region in such a way that minimized any energy transient in the system. This prevents the ice from melting and the peptide conformation from being influenced by a temperature "spike" during equilibration. This was accomplished by removing water molecules that overlapped with any peptide atom and then performing 20 steps of steepest descents energy minimization and 100 steps of conjugate gradient energy minimization on the peptide-interface system. The resulting system is shown in Figure 1, where it can be seen that the AFP molecule has some contacts with the rough surface of the solid.

The complete system, containing one AFP molecule placed at the ice/water interface, was allowed to equilibrate for 28 ps, after which 72 ps of production dynamics were performed. The average temperature of the system over the production period was 203 K. There was no overall drift in the magnitude of the total electrostatic and total van der Waals energies during the production dynamics. The equilibration of the peptide structure was followed by determining the root-mean-square deviations of the positions of all the atoms in the AFP as a whole, as well as those of the backbone atoms and those of the side chains. The rms deviations for each of the three groupings of peptide atoms reached stable values by 15 ps. The rms deviations values of 1.0, 1.3, and 0.8 Å for all, side chain, and backbone atoms were much lower (2–3 Å) than the corresponding values for the simulations of the wild-type AFP in water (McDonald et al., 1993). This is due to the lower thermal energy in this low temperature system.

This 100-ps simulation required about 83 CPU-hours on a Cray C-90 "supercomputer." An equivalent length of simulation on an IBM RS/6000-350H would take roughly 800 CPU-hours.

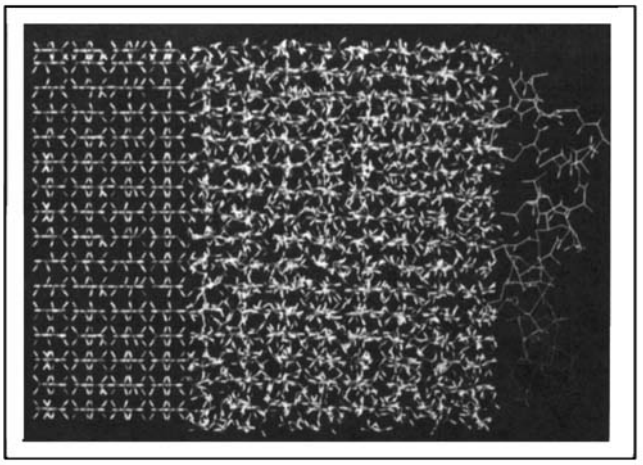

Figure 1. AFP molecule following energy minimization near an ice/water interface with an exposed $(20\bar{2}1)$ face.

The four leftmost layers of ice compose the fixed lattice; the remaining water molecules shown constitute the dynamic ice and part of the interface. The water molecules originally in the liquid region have not been drawn. The peptide can be seen to be bound at the curled C-terminus (near the top of the photo) and through an Arg residue nearby. Part of the midsection of the peptide, near Leu 12, sits in a cavity in the ice.

Effect of Peptide on the Ice/Water Interface

The morphology of the ice/water interface was studied by Haymet and coworkers for two different rigid water models, the well-known TIP4P and SPC potentials (Karim et al., 1990; Karim and Haymet, 1988). These studies showed the ice/water interface to be diffuse, spanning about three molecular layers (about 10 Å). The temperature below which the ice no longer melted was found to be 240 and 200 K for the TIP4P and SPC models, respectively. Like Haymet and coworkers, we determined the position of the interfacial region during the MD simulation using two-dimensional density profiles and diffusion coefficients traversing the system

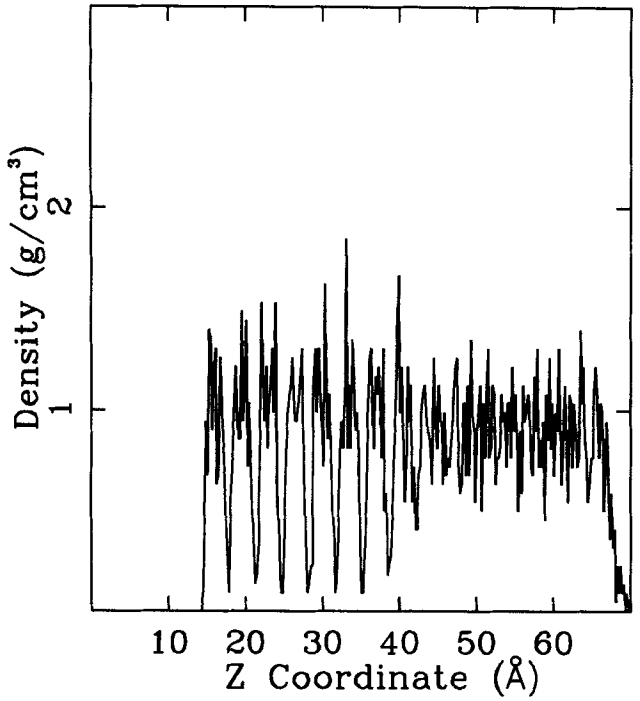

Figure 2. Density profile for the equilibrated [20$\bar{2}$1] ice/water interface prior to insertion of the peptide.

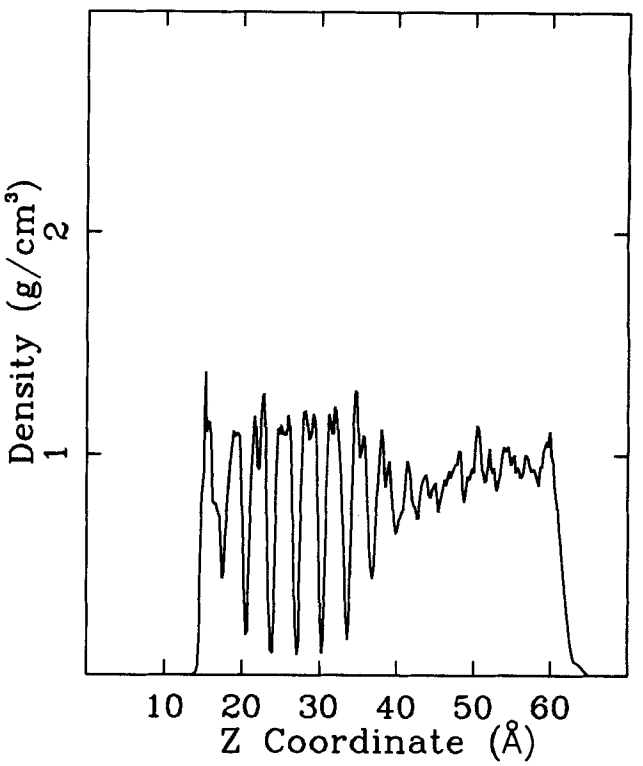

Figure 3. Density profile for the [20$\bar{2}$1] ice/water interface after insertion of the peptide, averaged over the interval from 92 to 100 ps.

Note that the presence of the peptide in the region from 40 to 48 Å causes a decrease in the density of the water due to its exclusion near the AFP.

from the solid region to the bulk liquid, thus locating the interface between these two phases.

The oxygen-atom density profiles across the ice/water interface in the z-direction were determined by averaging over 8 ps. Averages over 1 ps gave profiles with qualitatively similar features. Six strong peaks corresponding to bulk ice were apparent in the density profile, two peaks of intermediate height with nonzero minima were due to the interfacial region, and a section having a density just below 1.0 g/cm^3 corresponded to the bulk liquid water phase of the system. Originally, the ice contained eight molecular layers, thus the last two layers of ice and the nearby region of the liquid had formed the interfacial region during the equilibration of the ice/water interface (Figure 2). Equilibration of the ice/water system proceeded until the position of the interface was immobile, which was established rapidly, after about 4 ps. In fact, no movement of the interface was observed even after the peptide was inserted and throughout the entire production run, see Figure 3. Thus the ice neither melted nor grew during the simulation at 200 K, as one would expect of a system at its melting point. The interface here consisted of 2–3 molecular layers, similar to the results for the basal plane studied by Haymet et al. (Karim et al., 1990).

The self-diffusion coefficients for water molecules in each 3.4-Å-wide molecular layer were found by averaging over results for 4 ps, following the procedure of Haymet. We observed that the mean squared displacement values were linear over this period and that the diffusion did not change appreciably if the observation time were halved. The diffusion coefficient for SPC water at an ice/water interface at 200 K was found to be 0.3×10^{-5} cm$^2\cdot$s^{-1} by Karim et al. (1990). The analysis was based on the z-coordinate of the oxygen atoms at each instant in the trajectory and the mean-squared displacement calculated for a 4-ps time period.

The slope of the linear portion of each mean-squared displacement curve was used to determine the diffusion coefficients for the water molecules in each molecular layer. The ice portion of the system had a diffusion coefficient $< 0.05\times 10^{-5}$ cm^2/s. The interface displayed diffusion coefficients in the range $0.05–0.15\times10^{-5}$ cm^2/s. The liquidlike layers had diffusion coefficients around 0.5×10^{-5} cm^2/s. This value is roughly half that calculated by Karim and Haymet (1988) for an equivalent region in the TIP4P-modeled ice/water interface. This is in accord with the known differences in the diffusion coefficients for TIP4P and SPC models. In comparison to the profiles by Karim and Haymet (1988), the progression of the diffusion coefficients traversing from the solid to the liquid was not as regular in shape, but the width of the interfacial region was around 10 Å, similar to that found in the Karim and Haymet study. The unchanging nature of these diffusion coefficients with time support the results from the density profiles that the ice/water interface was stable during equilibration. Later inclusion of the peptide near the interface did not lead to any melting of the ice. Thus, the peptide had no large-scale influence on the ice/water interface in terms of its ability to melt the ice at 200 K.

Polypeptide-Interface Interactions

Analysis of the interactions of the AFP molecule with wa-

ter molecules in the ice/water interface was used to determine the nature of any adsorptive contact with the interfacial region. These contacts might involve the formation of hydrogen bonds with water molecules in the interfacial section, interactions of the dipoles of water molecules in the ice with those of nearby groups on the peptide (such as the two charged terminuses), and van der Waals contacts of the nonpolar side chains of the AFP with the irregularly structured, dynamically changing interface. We shall now examine each of these possibilities.

Peptide-ice hydrogen bonding

The hydrogen bonds that occurred between the side chain and main chain groups of the wild-type peptide and water molecules were determined for each snapshot in the saved coordinate trajectory. A hydrogen bond donor-acceptor distance cutoff of 3.5 Å and a donor-hydrogen-acceptor angle cutoff of 120° were applied in examining the peptide/water hydrogen bonding. Any hydrogen bonds formed to water molecules that originally constituted part of the ice were considered contacts to the ice. Those that formed between peptide and any water molecules originally part of the liquid water side of the interface were counted as peptide/water contacts. Some water molecules in the interface underwent exchange between being in the more solidlike region of the interface to being in the more liquidlike region. However, the flux between the icelike and liquidlike water molecules in the interface was roughly equal, which effectively cancels any incorrect counting of peptide/ice and peptide/liquid hydrogen bonds, especially when averaged over the entire production period of the simulation.

The number of peptide/water hydrogen bonds in the system increased as the simulation proceeded, rising from 29 to 75 in 100 ps. Details of these 75 hydrogen bonds are summarized in Tables 1 and 2. This number is about 16 hydrogen bonds larger than was observed for the wild-type peptide in either SPC-modeled (McDonald et al., 1993) or TIP3P-modeled water (McDonald, 1995). There were about 59 peptide/liquid water interactions intact at any given instant and 16 peptide/ice hydrogen bonds. Thus the increase in peptide/water hydrogen bonds over those for the hydration of the peptide could be due to contacts to the ice, reflecting the preference of the peptide to bind to the ice. Alternatively, the larger number of peptide/water hydrogen bonds could have been due to an increased tendency for hydrogen

Table 1. Hydrogen Bonding of the AFP to (20$\bar{2}$1) Ice/Water Interface during the Period 28–100 ps*

Group Name	Total Hydrogen Bonds	Hydrogen Bonds to Solid	Hydrogen Bonds to Liquid
Asp 1 N-HT1	1.1	0.6	0.5
Asp 1 N-HT3	1.0	1.0	0.0
Asp 1 OD1	0.7	0.3	0.4
Asp 1 OD2	2.8	1.8	1.0
Asp 1 O	1.2	0.0	1.2
Thr 2 N-H	0.8	0.0	0.8
Thr 2 OG1-HG1	2.5	0.0	2.5
Thr 2 O	1.9	0.0	1.9
Ala 3 N-H	0.8	0.0	0.8
Ala 3 O	1.1	0.0	1.1
Ser 4 N-H	0.9	0.0	0.9
Ser 4 OG-HG	2.8	0.0	2.8
Ser 4 O	1.0	0.0	1.0
Asp 5 OD1	2.9	1.4	1.5
Asp 5 OD2	1.7	0.0	1.7
Asp 5 O	0.6	0.1	0.5
Ala 6 N-H	0.3	0.0	0.3
Ala 6 O	1.0	0.0	1.0
Ala 7 O	0.9	0.0	0.9
Ala 8 O	1.0	1.0	0.0
Ala 9 N-H	0.1	0.1	0.0
Ala 9 O	1.0	0.0	1.0
Ala 10 O	0.9	0.0	0.9
Ala 11 O	1.0	0.0	1.0
Leu 12 O	0.6	0.6	0.0
Thr 13 OG1-HG1	2.5	0.0	2.5
Thr 13 O	0.7	0.0	0.7
Ala 14 O	0.8	0.0	0.8
Ala 15 O	0.4	0.4	0.0
Asn 16 OD1	1.3	0.7	0.6
Asn 16 ND2-HD21	0.9	0.7	0.2
Asn 16 ND2-HD22	0.9	0.7	0.2
Asn 16 O	1.0	0.0	1.0
Lys 18 NZ-HZ1	1.5	0.0	1.5
Lys 18 NZ-HZ2	0.2	0.0	0.2
Lys 18 NZ-HZ3	1.0	0.0	1.0

*Values for residues 1–18 are shown, with the exclusion of groups forming no hydrogen bonds to water molecules.

Table 2. Hydrogen Bonding of the AFP to a (20$\bar{2}$1) Ice/Water Interface during the Period 28–100 ps*

Group Name	Total Hydrogen Bonds	Hydrogen Bonds to Solid	Hydrogen Bonds to Liquid
Ala 19 O	1.5	1.1	0.4
Ala 20 O	2.1	0.0	2.1
Glu 22 OE1	3.8	0.0	3.8
Glu 22 OE2	2.0	0.0	2.0
Glu 22 O	1.1	0.0	1.1
Thr 24 OG1-HG1	0.4	0.0	0.4
Ala 25 N-H	0.1	0.0	0.1
Ala 25 O	1.0	0.0	1.0
Ala 26 O	1.0	0.0	1.0
Asn 27 OD1	0.5	0.0	0.5
Asn 27 ND2-HD21	1.0	0.0	1.0
Asn 27 ND2-HD22	1.6	0.0	1.6
Ala 28 O	1.0	0.0	1.0
Ala 29 O	1.7	0.0	1.7
Ala 30 O	2.1	0.0	2.1
Ala 32 N-H	0.9	0.0	0.9
Ala 32 O	1.7	0.0	1.7
Ala 33 N-H	0.1	0.1	0.0
Ala 33 O	1.8	1.7	0.1
Ala 34 O	1.1	0.0	1.1
Thr 35 OG1-HG1	1.0	0.0	1.0
Thr 35 O	0.8	0.0	0.8
Ala 36 N-H	0.9	0.0	0.9
Ala 36 O	2.3	2.3	0.0
Arg 37 OCT2	1.9	1.9	0.0
Total	75.1	16.5	58.6

*Values are given for residues 19–37, with the exclusion of groups forming no hydrogen bonds to water molecules.

bonds to form at the lower temperature in this simulation (200 K here vs. 300 K in the hydration simulation). A further higher temperature simulation of the peptide/water/ice system would be necessary to determine if the latter explanation is valid.

The residues found to have formed hydrogen bonds to the icelike interfacial region included the amino and carboxy terminuses, the side chains of Asp 1, Asp 5, and Asn 16, along with the main chain carbonyl groups of Ala 8, Leu 12, Ala 15, Ala 19, Ala 33, and Ala 36. None of these hydrogen bonds between the ice and main chain carbonyl groups existed at the start of the simulation. When we compared the binding formed in the rather constrained "docking" minimization procedure and the unconstrained MD simulation of the ice/water interfacial system, we found considerable differences. In the "docking," the only group of the peptide that was hydrogen bonded to water molecules in the ice slab was the main chain carbonyl of Ala 36, which formed two hydrogen bonds with water molecules. The peptide in the interfacial system had the same orientation as in the docking study, but here it preferred to form numerous hydrogen bonds to water molecules in the interfacial region, through its side chains and some main chain groups. Thus the shape of the peptide formed a better "fit" with the rough $(20\bar{2}1)$ interface than the "docked" peptide at a bare ice surface. This can be seen in Figure 4, which shows Quanta-generated photographs of the peptide-interface system following 100 ps of MD simulation. Several side chain and main chain groups of the peptide, including the *N*- and *C*-terminuses, have formed new associations with the irregularly shaped interfacial region.

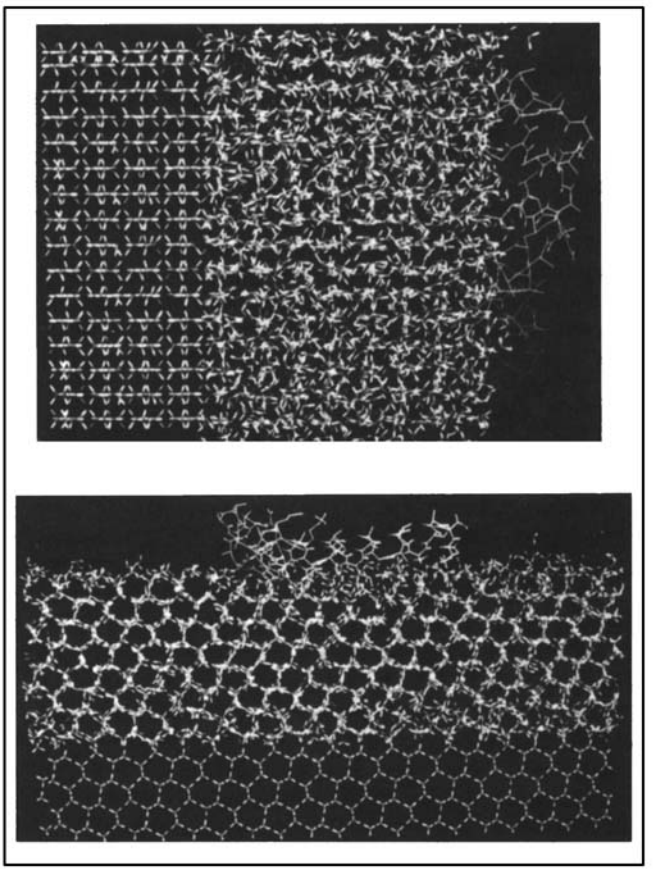

Figure 4. Two views of the AFP molecule following 100 ps of MD near an ice/water interface.

Key as in Figure 1. Note the increased number of contacts between the ice and the peptide in comparison to Figure 1.

Peptide-water hydrogen bonding

Hydrogen bonding interactions of the peptide with water molecules in the liquid phase of the interface could also be important to the function of the AFP molecule in stopping ice growth. One proposed mechanism suggests that the peptide might act by influencing the translational mobility and three-dimensional structuring of water molecules and thus interfere with the process by which water molecules in the liquid gain access to and join the solid phase (Feeney et al., 1986). In the hydration study (McDonald et al., 1993), the diffusion of water molecules near polar groups of the peptide that contained oxygen atoms was reduced by a factor of 3 relative to that in the bulk solvent, which may allow water structuring for a longer lifetime.

The number of hydrogen bonds that each group of the wild-type polypeptide formed with water molecules considered to be in the liquid phase, using the classification method described earlier for the peptide/ice hydrogen bonds, are shown in the last columns of Tables 1 and 2. The number of hydrogen bonds to water for the hydroxyl-containing side chains of Thr 2, Ser 4, and Thr 13 was slightly larger than in the hydration. This may be due to the increased tendency for hydrogen bonds to form at lower temperatures. The side chains of Thr 24 and Thr 35 formed fewer hydrogen bonds to the liquid in the interfacial simulation as compared to the hydration; instead they satisfied part of their hydrogen bonding capacity by interacting with main chain carbonyl groups, as is discussed in subsection titled "Peptide/peptide interactions." Main chain groups behaved similarly in both the hydration and interfacial simulations.

For most of the main chain carbonyl groups of the peptide, hydrogen bonding was exclusively to the liquid-phase water molecules and involved about one such hydrogen bond. An exception was observed for the carbonyl of Ala 20, which entered into two hydrogen bonds on average with water molecules in the liquid phase. This carbonyl group did not fulfill one of its hydrogen bonds by interacting with the side chain of Thr 24, as in the hydration study, and might be more available to interact with ice if the peptide rotates around its long axis. The side chain of Thr 24 formed a hydrogen bond to Ala 19 instead (as in the initial configuration). Hydrogen bonding interactions were rarely observed between main chain amide groups and water molecules in the liquid portion of the interface. Fewer hydrogen bonds to the liquid were found for the amino-terminus and the side chains of Asp 1, Asp 5, and Arg 37 for the interfacial system as compared to the hydration. Even though these groups were hydrogen bonded to the ice, they showed fewer hydrogen bonds to water molecules overall in comparison to the hydration study. This is probably related to the steric hindrance provided by the ice. In particular, the side chain of Arg 37 showed no hydrogen bonding to water molecules in either the liquid, in-

terfacial, or ice regions. Instead, this side chain hydrogen bonded to several main chain groups, as described in subsection titled, "Peptide/peptide interactions." The carboxy terminus also had a different pattern of hydrogen bonding in this interfacial study, preferring to form about two hydrogen bonds to the interfacial region instead of several hydrogen bonds to liquid water in hydration. Despite the small differences noted previously, the peptide/water interactions in this interfacial simulation were similar to those in bulk water. Thus, the presence of the ice did not significantly influence the mobility or ordering of nearby water molecules in the liquid compared to its hydration conformation.

Elastrostatic and van der Waals interactions

The results of Lal et al. (1993) agreed with the experimental hypothesis that the wild-type polypeptide interacts more strongly with the $(20\bar{2}1)$ ice plane compared to the basal or prism planes. They related this difference to the formation of a more intimate contact of many parts of the peptide with the rougher $(20\bar{2}1)$ plane and found that the van der Waals component of the energy was more negative for the $(20\bar{2}1)$ face compared to the basal plane. We found that the van der Waals component increased (became less favorable) by about 10% during the equilibrium period, but remained constant after that, as shown in Figure 5. The corresponding history for the electrostatic energy component, seen in Figure 6, showed a decrease of larger magnitude over a similar timescale. This suggests that improved electrostatic interactions developed at the expense of some unfavorable steric ones. However, our docking studies did not clearly show a preference for the peptide to bind to one particular ice face.

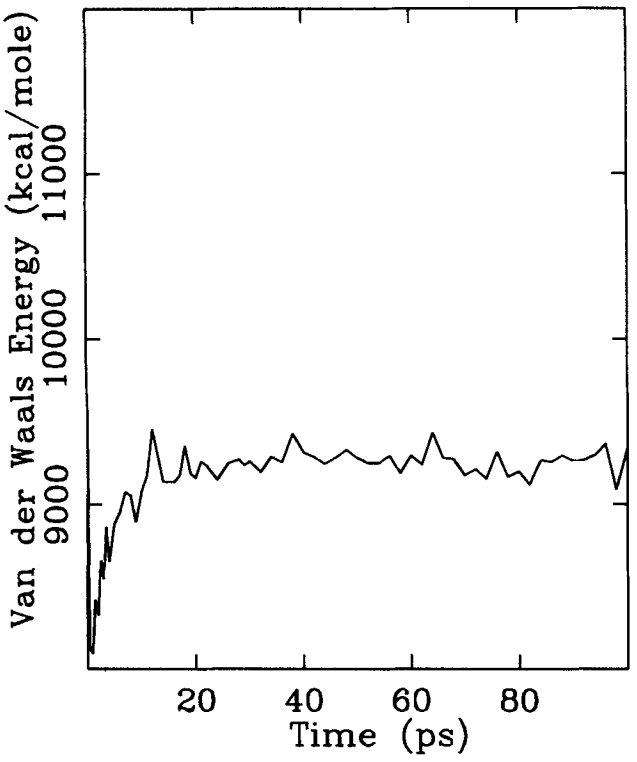

Figure 5. History of the van der Waals energy for the AFP near a [20$\bar{2}$1] ice/water interface.

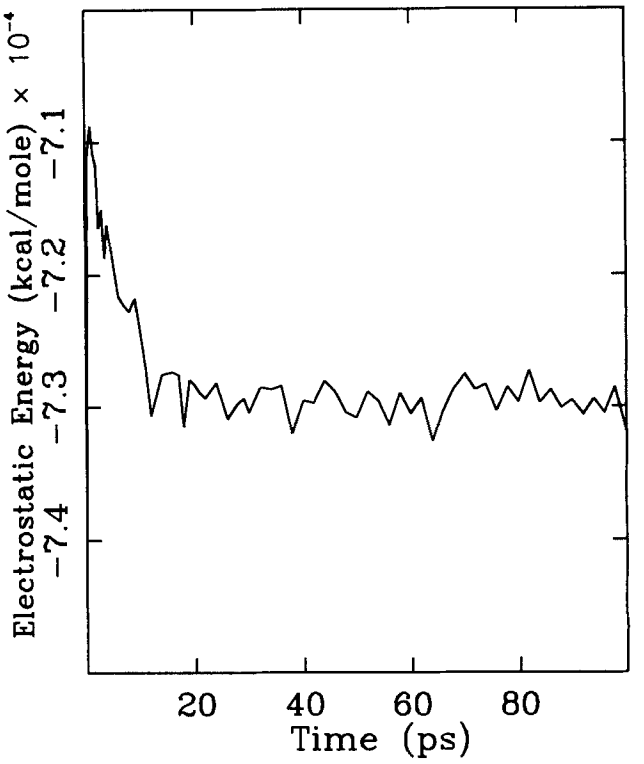

Figure 6. History of the electrostatic energy for the AFP near a [20$\bar{2}$1] ice/water interface.

Effect of the Ice on the Polypeptide

The effect of the presence of the ice/water interface on the peptide itself was also studied, for example, to determine any loss of helicity or change in helix bending. The mechanism by which the peptide is effective in stopping ice growth may involve the formation of secondary contacts to the interfacial region, following the initial contact by polar groups. Formation of these secondary contacts may be facilitated by changes in the extent of the helix bend, the conformation of the side chains and backbone, and shifts in the pattern of peptide/peptide hydrogen bonding vs. peptide/water (liquid or solid) hydrogen bonding.

Peptide conformation

The average conformation of the main chain and the side chains of the wild-type AFP near the ice/water interface was determined. Using ϕ and ψ angles to refer to rotation around the N-C_α and C_α-C bonds of each residue, involving 4 contiguous backbone atoms in the definition of each angle in Table 3, it can be seen that 25 of the 35 interior residues remained helical, using a 15° window about the α-helical values of $-67°$ and $-44°$ of ϕ and ψ, respectively. A picture of the peptide near the ice/water interface following 100 ps of MD is shown in Figure 7. The peptide was much less helical

Table 3. Average Dihedral Angles for the AFP Near a (20$\bar{2}$1) Ice/Water Interface at 200 K over the Interval 28–100 ps

Residue	ϕ	ψ	ω	χ_1	χ_2	χ_3	χ_4	χ_5	χ_6	χ_7
Asp 1	—	−164.7	−179.5	64.3	33.6					
Thr 2	−57.7	−51.3	−175.8	−48.7	−90.7					
Ala 3	−147.7	−21.0	−176.4							
Ser 4	−65.6	−33.9	175.5	−47.6	43.2					
Asp 5	−65.7	−35.6	173.8	62.1	155.4					
Ala 6	−60.8	−41.1	176.4							
Ala 7	−63.3	−42.3	−179.7							
Ala 8	−65.2	−46.9	174.7							
Ala 9	−58.9	−35.6	176.5							
Ala 10	−62.1	−34.4	174.4							
Ala 11	−63.5	−36.2	175.3							
Leu 12	−65.8	−42.7	177.7	−54.8	−61.3					
Thr 13	−57.7	−38.8	175.2	−48.5	69.6					
Ala 14	−59.8	−44.8	178.4							
Ala 15	−63.7	−38.1	174.7							
Asn 16	−57.6	−44.0	176.5	178.8	−51.0	−177.6				
Ala 17	−63.4	−36.3	−176.4							
Lys 18	−59.3	−48.8	176.8	−70.6	−68.2	−178.9	−59.1	−169.4		
Ala 19	−67.6	−27.7	178.4							
Ala 20	−70.5	−45.4	−177.2							
Ala 21	−148.0	−47.7	−168.0							
Glu 22	−56.8	−58.1	−178.2	−53.5	175.8	−172.5				
Leu 23	−80.9	−29.8	178.1	−171.3	−178.7					
Thr 24	−83.4	−89.0	−170.2	47.0	−175.3					
Ala 25	−54.0	−51.6	−179.5							
Ala 26	−65.4	−47.5	−177.0							
Asn 27	−73.3	−21.7	174.0	−166.7	−121.6	−174.2				
Ala 28	−70.2	−32.4	171.5							
Ala 29	−63.9	−37.9	176.9							
Ala 30	−66.6	−39.0	176.8							
Ala 31	−164.4	92.6	176.3							
Ala 32	−77.5	138.6	−176.6							
Ala 33	58.2	50.5	179.4							
Ala 34	−156.7	−72.5	−176.0							
Thr 35	−83.6	80.0	−175.1	39.8	−172.6					
Ala 36	71.1	−19.4	173.0							
Arg 37	−163.1	—	—	46.0	80.5	−64.4	−79.6	169.3	176.9	173.4

than in our hydration study, in which 33 of the interior residues were helical on average (McDonald et al., 1993). The nonhelical residues included Thr 2, Ala 3, Ala 21, Thr 24, and Ala 31–Ala 36, most of which were hydrogen-bonded to the liquid. These same residues were nonhelical in the starting peptide structure selected from the *in vacuo* trajectory. As in the hydration study, the ω angle of Ala 21 was much lower than those of surrounding residues, showing that a twist existed in the peptide at the center of the bend. The noted lack of helicity for Thr 24 was due to a low value of its ψ angle, a feature that was also found in the peptide structure used to start the simulation. The bend in the center of the peptide was maintained in part during the simulation by this additional (compared to the hydration) nonhelical residue near the Lys–Glu salt bridge. These results for the backbone dihedral angles indicate that the wild-type AFP remained mostly helical in the vicinity of the ice/water interface, with the nonhelicity concentrated at the ends (especially the carboxy terminus) and near the salt bridge in the middle of the peptide.

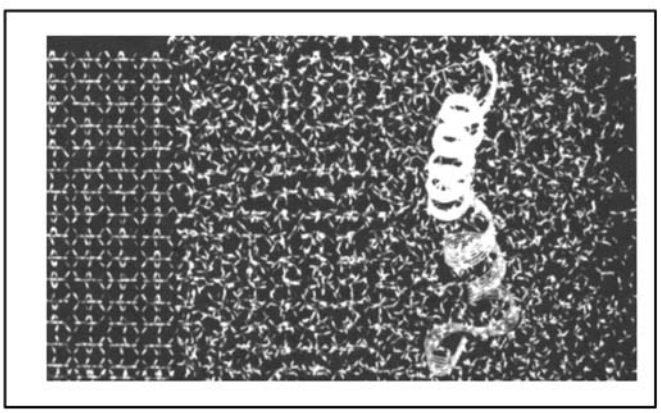

Figure 7. AFP molecule and the entire ice/water system following 100 ps of MD.

A ribbon diagram has been fitted to the backbone atoms of the peptide. Note the uncurled conformation of the carboxy-terminal end of the peptide.

The conformation of the wild-type peptide was also investigated by obtaining histories of the main chain and side chain dihedral angles over the course of the entire simulation. No residues underwent transitions of lasting significance. The rms fluctuations in the main chain dihedral angles were less than 10° in most cases, with the exceptions being residues on the ends of the peptide. The histories of the backbone dihedral

angles also indicate that the helical structure of the peptide was maintained, with no further loss of helical structure over the hydration study.

Side chain motions

The average values for the side chain χ angles are given in Table 3. The arrangement of many of the side chains was different from that observed in the hydration study, except for Thr 2, Leu 12, and Glu 22. The Thr 24 and Thr 35 side chains differed in conformation for both their χ_1 and χ_2 angles. The side chains of the terminal residues were not in an extended arrangement here (χ_1 values near $\pm 180°$), as they were in the hydration. The ice/water interface provided a different environment for the side chains causing transitions in the dihedral angles of the side chains in order to reestablish the balance between peptide/water and peptide/peptide interactions. A search for such side chain rotations was made by examining the histories of the side chain dihedral angles over the entire simulation. Some of the side chains underwent transitions of 30° or more in the values of one or more of their side chain dihedral angles (see Table 4).

The hydroxyl-containing side chains, except for Thr 35, underwent substantial motions, with transitions typically occurring several times over the 100-ps simulation. As shown in the analysis of peptide/water hydrogen bonding presented earlier, these side chains interacted only with water molecules in the liquid section of the interface. Rotation about the chemical bonds of the side chains was preceded by breakage of the corresponding side chain to water hydrogen bond and was followed by reformation of hydrogen bonds to solvent, but with the side chain arranged differently relative to the main chain of the peptide. Often, these changes in the orientation of the side chain were short-lived and the side chain returned to its original conformation.

The magnitude of the transitions in conformation were of the order of 60° to 180° and their frequency was generally less than that observed for the wild-type AFP in bulk water. The more mobile side chains were oriented into the liquid portion of the system and would have been expected to have similar motions to those seen in the hydration. Here, the lower temperature resulted in a partial loss of side chain mobility. These results suggest that the side chains of the AFP undergo motions often enough and to an extent that might allow for the formation of additional contacts between the peptide and the interfacial region, but the computational cost of

Table 4. RMS Fluctuations in Dihedral Angles for the AFP Near a (20$\bar{2}$1) Ice/Water Interface at 200 K

Residue	ϕ	ψ	χ_1	χ_2	χ_3	χ_4	χ_5	χ_6	χ_7
Asp 1	—	7.7	56.2	7.1					
Thr 2	10.3	10.6	13.1	67.9					
Ala 3	11.5	10.9							
Ser 4	9.5	9.1	10.0	86.6					
Asp 5	7.0	6.8	34.2	8.1					
Ala 6	6.7	6.9							
Ala 7	6.7	7.2							
Ala 8	6.6	6.1							
Ala 9	6.6	6.5							
Ala 10	6.2	7.0							
Ala 11	5.8	6.9							
Leu 12	6.5	5.8	8.3	10.4					
Thr 13	6.3	5.8	6.6	55.9					
Ala 14	6.7	6.8							
Ala 15	6.6	6.8							
Asn 16	6.8	6.3	23.8	26.0	6.4				
Ala 17	6.5	6.3							
Lys 18	6.0	6.2	6.4	8.5	8.8	8.9	14.0		
Ala 19	6.7	7.3							
Ala 20	7.5	11.7							
Ala 21	10.6	9.4							
Glu 22	7.6	7.8	8.2	7.6	46.7				
Leu 23	8.2	6.8	12.6	8.6					
Thr 24	7.7	9.0	6.7	18.6					
Ala 25	9.4	7.8							
Ala 26	6.9	7.2							
Asn 27	6.3	6.8	5.6	9.0	6.2				
Ala 28	7.0	6.7							
Ala 29	6.5	7.8							
Ala 30	8.2	11.0							
Ala 31	8.4	16.3							
Ala 32	10.6	9.6							
Ala 33	6.4	10.0							
Ala 34	8.9	10.3							
Thr 35	8.1	5.8	7.5	12.5					
Ala 36	6.1	13.2							
Arg 37	14.9	—	6.0	6.5	6.2	7.2	5.5	6.7	6.5

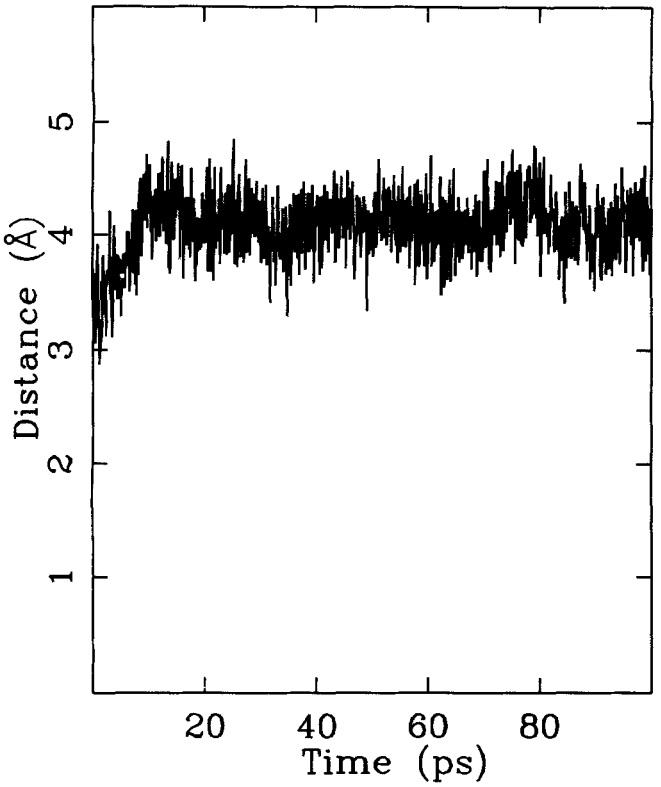

Figure 8. Time series of the distance between the main chain carbonyl oxygen atom of Glu 22 and the main chain amide nitrogen atom of Ala 26 of the AFP.

the simulation precluded simulating the system for long enough to confirm this.

Peptide/peptide interactions

Peptide/peptide hydrogen bonds were also found to stabilize the helical structure of the AFP molecule here, as found in the vacuum and hydration studies we have carried out. Hydrogen bonds were characterized by a donor-acceptor distance cutoff of 3.5 Å and a donor-hydrogen-acceptor angle cutoff of 120°. Main chain hydrogen bonds of the typical (i, $i+4$) type for a helix were broken most of the time in bonds numbered 1, 2, 19, 20, 23, 29, 30, 32, and 33. In this number scheme, the bond number corresponds to the index i, with the carbonyl of residue i forming a hydrogen bond with the amide of residue $i+4$. Bond number 18 was intact most of the time, but had two breakages lasting 10 ps each. Bond number 22 between Glu 22 and Ala 26 was intact early in the simulation and then separated permanently, as shown by the history of the O–N distance (see Figure 8). This is the same pattern as for the *in vacuo* simulation at 300 K. Thus, the stabilization of the peptide backbone by the main chain hydrogen bonds in the middle of the molecule was lost throughout this current simulation, a loss that also developed during the 300 K vacuum simulation. The implications of this continuing pattern of backbone hydrogen bonding on the helix bending motion that was observed *in vacuo* at 300 K will be discussed in the following subsection.

Table 5. Number of Transitions in Selected Side Chain Dihedral Angles of the AFP at an Ice/Water Interface at 200 K

Residue	Atoms in Dihedral	No. of Transitions
Asp 1	ca-cb-cg-od1	6
Thr 2	n-ca-cb-og1	1
Thr 2	ca-cb-og1-hg1	12
Ser 4	ca-cb-og-hg	16
Asp 5	ca-cb-cg-od1	1
Thr 13	ca-cb-og1-hg1	3
Lys 18	cd-ce-nz-hz1	4
Glu 22	cb-cg-cd-oe1	1
Thr 24	ca-cb-og1-hg1	6
Asn 27	ca-cb-cg-od1	1
Thr 35	ca-cb-og1-hg1	0

A search for hydrogen bonding interactions of the side chains of the peptide with the main chain was also made by determining donor-acceptor distance histories. The geometries for these interactions for the average production structure of the peptide are shown in Table 5. The side chain of Asp 5 (containing a charged carboxyl group) interacted strongly with the amino terminus, in a salt bridge. The charged side chain of Arg 37 was involved in a salt-bridge interaction with the carboxy terminus. These two interactions have the effect of reducing the side chain interactions with the helix macrodipole. The overall dipole moment of the helix arises from the charged terminuses together with the unpaired main chain groups on the ends of the peptide in the (i, $i+4$) main chain hydrogen bonding pattern. These salt-bridge interactions are thought to make the molecule more stable in polar solvents such as water. As in the vacuum and hydration simulations, the ends of the peptide "curled" around to allow the formation of interactions between the side chains of the terminal residues and the main chain. The extent of the "curling" on the carboxy terminal end of the peptide was sufficient to allow the formation of a hydrogen bond with the side chain of Asn 27, three helical turns away in the sequence. Similar curled terminuses have been observed experimentally, a phenomenon known as "capping" (Stickle et al., 1992). As noted previously, the Arg 37 side chain did not form hydrogen bonding interactions to water molecules either in the liquid or solid regions of the interface. Similar to the hydration studies, the side chains of Thr 13, Thr 24, and Thr 35 were in close association with their respective main chain amide groups, but the angle of these interactions precluded their inclusion as hydrogen bonds.

The only threonine group that regularly satisfied the hydrogen bond cutoff angle was the Thr 24 side chain bonded to the main chain amide of Ala 25. Unlike our previous simulations of the AFP, the carboxy terminus interacted in a hydrogen bonding manner with main chain peptide groups, in this case the amide groups of Ala 33 and Ala 34. The peptide was curled near its carboxy terminus in the starting coordinates for this MD simulation, with the same two terminus-amide hydrogen bonds being intact. The interaction of the side chain of Thr 24 with main chain carbonyl groups was again observed. The hydrogen bond to the carbonyl of Ala 19 was intact over the entire simulation, while the hydrogen bond to the carbonyl of Ala 20 was formed only a small fraction of the time (see Figure 9). In the hydration study, the hydrogen

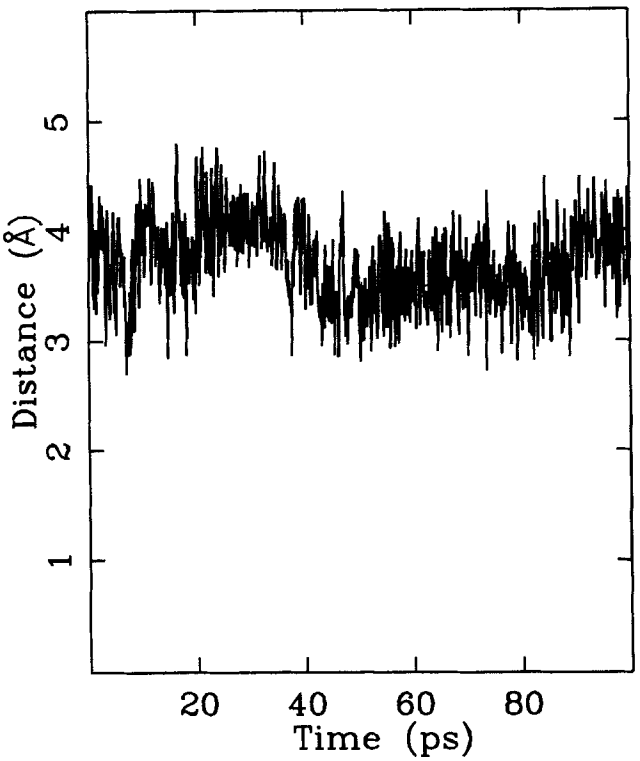

Figure 9. History of the distance between the side chain hydroxyl oxygen atom of Thr 24 and the main chain carbonyl oxygen atom of Ala 20 of the AFP.

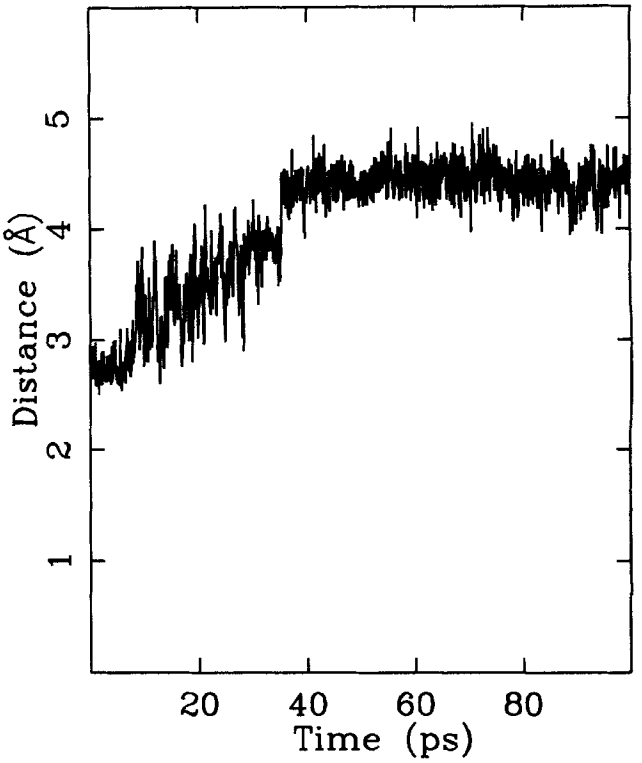

Figure 10. History of the distance between the side chain amino nitrogen atom of Lys 18 and the side chain carbonyl oxygen atom (OE1) of Glu 22 of the AFP.

bond of the Thr 24 side chain with the carbonyl of Ala 20 was intact, while here, as in the initial configuration, the hydrogen bond to the carbonyl of Ala 19 predominated.

In the 300 K vacuum study of the wild-type peptide (McDonald et al., 1993), the side chain of Thr 24 changed the main chain carbonyl group to which it was hydrogen bonded; this event was thought to be crucial in the development of the helix bend. Since the same pattern of side chain to main chain hydrogen bonding in the center of the peptide was maintained throughout this simulation, we expect the helix bend angle to be maintained, as discussed below.

There were a few side chain to side chain interactions from the starting structure that were intact in the peptide during this interfacial simulation. The salt bridge between the side chains of Lys 18 and Glu 22 was present at all times. The charge/charge type of interaction involved in the salt bridge is a stronger interaction than a hydrogen bond. One of the two oxygen atoms of Glu 22 slowly drifted away from the amino group on the end of the lysine side chain to a distance of about 4.5 Å as shown in Figure 10, but remained close enough to interact strongly with the charged amino group.

The only other hydrogen bond among the side chains that remained largely intact occurred between the hydroxyl group of Thr 35 and one of the amino groups of Arg 37 (see Table 6). Average geometries and distance histories indicate that the helix in this system was stabilized by the same types of intramolecular hydrogen bonds, together with a few charge/dipole and charge/charge interactions, as for the peptide modeled in bulk water. The extent of intactness of the main chain hydrogen bonds was similar in the bulk liquid and interfacial environments, but there were differences in the side chain to main chain hydrogen bonding.

Table 6. Geometry for Peptide-Peptide Hydrogen Bonds of the AFP Near a (20$\bar{2}$1) Ice/Water Interface at 200 K

Donor Group	Acceptor Group	Avg. Distance (Å)	Avg. Angle (deg)
Asp 1 N-HT2	Asp 5 OD1	3.14	127
Asp 1 N-HT2	Asp 5 OD2	3.22	168
Asp 5 N-H	Asp 1 OD1	3.16	155
Ala 6 N-H	Asp 5 OD2	3.02	128
Thr 13 N-H	Thr 13 OG1	2.67	100
Lys 18 NZ-HZ2	Glu 22 OE2	2.72	158
Thr 24 N-H	Thr 24 OG1	2.65	105
Thr 24 OG1-HG1	Ala 19 O	2.81	151
Ala 25 N-H	Thr 24 OG1	2.94	128
Ala 33 N-H	Arg 37 OCT1	2.96	123
Ala 33 N-H	Arg 37 OCT2	2.88	162
Ala 34 N-H	Arg 37 OCT1	2.92	178
Thr 35 N-H	Thr 35 OG1	2.66	104
Arg 37 NE-HE	Arg 37 OCT2	3.08	143
Arg 37 NH1-HH11	Thr 35 OG1	2.77	148
Arg 37 NH1-HH12	Ala 31 O	2.70	135
Arg 37 NH1-HH12	Arg 37 OCT1	2.82	121
Arg 37 NH2-HH21	Asn 27 OD1	2.69	145
Arg 37 NH2-HH22	Leu 23 O	2.74	142

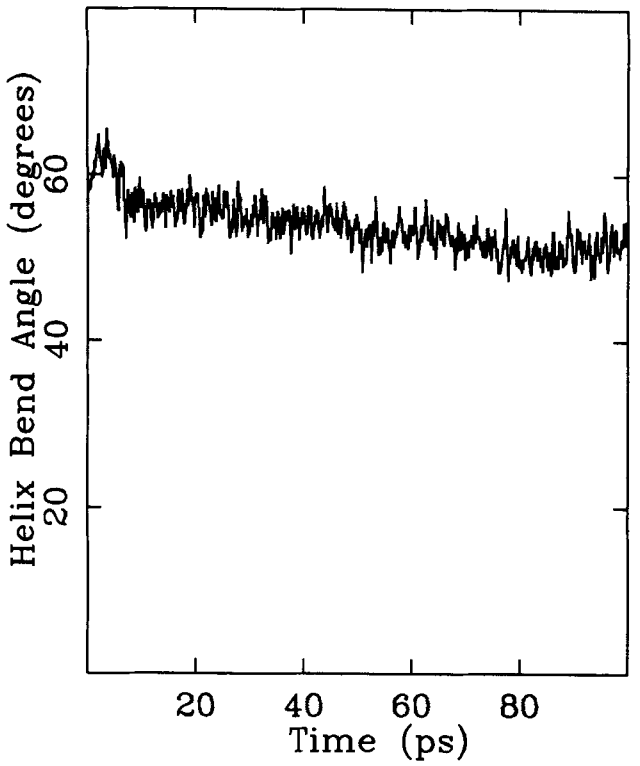

Figure 11. Time series of the helix bend angle of the AFP near a [20$\bar{2}$1] ice/water interface.

The vectors defining the angle ran between the C_α atoms of residues 5 and 16 residues 24 and 31.

Helix bending

The structure used to start the interfacial simulation had a bend angle of 58° as defined by the angle between vectors from the α-carbon groups of Asp 5 to Asn 16 and from Thr 24 to Ala 31. The history of the helix bend angle throughout the simulation is shown in Figure 11. A slight decrease in the bend angle occurred over the first 80 ps of the simulation, with the value of the angle changing from 58° to around 55°, after which the angle remained fairly constant. There were no large-scale oscillations of the bend angle, possibly due to the combined damping influences of the water molecules surrounding the AFP and the low temperature at which the simulation was conducted. As noted in the previous subsection, the pattern of main chain hydrogen bonding was nearly constant, and this feature is one possible explanation for the observed ability of the peptide to maintain its initial bend while near the ice/water interface. Due to the short observation time, the relatively constant behavior of the helix bend angle may be viewed as indicative of a preference for the peptide to remain in a bent shape near the [20$\bar{2}$1] ice/water interface or as a simulation constraint caused by these low-mobility conditions. There is an urgent need for molecularly detailed experimental (such as nmr) studies of the peptide in water and near ice to determine whether there is any significant bend in the helix.

Peptide translation and rotation

Examination of the conformation of the AFP throughout the simulation showed that no net translation or rotation of the peptide had occurred. Rotation of the peptide over the interface was probably hindered by the relatively small distance of the peptide from its periodic "image," though we were careful to ensure that the peptide was not within its influence. Translation, too, is unlikely due to the low diffusion coefficient of this peptide. Even in the higher temperature hydration simulation, the mobility of the peptide was more than an order of magnitude lower than that for water molecules in the bulk solvent. A "log-roll" rotation of the peptide about the long axis of the helix was not observed in the graphical animation; no change occurred as to which peptide groups were closest to the interfacial region.

The lack of net translation or rotation of the wild-type AFP in this study near a (20$\bar{2}$1) planar ice/water interface emphasizes the need to start the peptide in the orientation that is the most preferable for adsorption. At these low temperatures, the peptide may be unable to make a transition to another orientation on a timescale that can be examined using MD simulation. Peptide motion is further constrained by the strong interactions that some of the peptide groups formed with the interfacial region.

Conclusions

The first report of the interaction of a wild-type winter flounder AFP molecule with an ice/water interface was made using MD simulation techniques. Significantly increased contact was found between the peptide and surrounding water molecules in comparison to the behavior of the AFP in bulk water. This increased contact was entirely due to the formation of strong ice/peptide hydrogen bonds. The peptide interacted with the ice/water interface through a mixture of hydrogen bonds to both the liquid and solid phases. Peptide/water bonds were formed with all the threonine side chains (extended out into the liquid), and with other polar side chains and main chain carbonyl groups; about 59 hydrogen bonds were formed with the water molecules in the liquid. Sixteen peptide/ice hydrogen bonds were formed with the *C*- and *N*-terminuses, the side chains of Asp 5 and Asn 16, and the main chain carbonyl groups of Ala 8, Leu 12, Ala 19, Ala 33, and Ala 36. The total number of peptide/water hydrogen bonds was 75, showing a 20% increase over its value in bulk water at 300 K.

The peptide remained in a stable helical, somewhat bent, conformation throughout the simulation. The bent region of the peptide extended over a larger segment of residues (in the center of the helix) compared to the hydration. The bending decreased slightly throughout the run, though the simulation could not be run long enough to determine how straight it might become.

Two main differences were found in this ice/water system as compared to the ice/vacuum "docking" studies. First, the alteration in the extent of the bend only occurred in this ice/water system, not in the earlier *in vacuo*, hydration or "docking" studies. Since this bend—if real—could have important mechanistic implications, it may be that full ice interfacial systems are needed. Second, the degree of "fit" to the ice was enhanced in the interfacial system relative to the docking studies, which, again, may be important mechanistically.

Several pieces of mechanistic information have resulted from this simulation. First, positioning the peptide near the interfacial region did not cause melting of the ice at its ice point. This is consistent with an adsorptive mechanism in which the peptide kinetically retards ice growth rather than a simply colligative thermodynamic effect caused by the presence of the peptide in solution. This agrees with experimental findings. Second, in the proposed adsorption mechanism of Knight et al. (1991), the peptide was assumed to act by binding the four threonine side chain hydroxyl groups to water molecules in the ice phase. In this simulation, however, the threonine side chains were oriented *away from* the interfacial region throughout the simulation, as observed in a computer graphics animation of the system using QUANTA 3.4 (Molecular Simulations, 1992), yet the peptide was still able to form strong contacts with the ice. This suggests that binding by the polar Thr groups may not be the only way for peptides to successfully bind to ice surfaces, and hence other mechanistic pathways may be possible strategies for antifreeze activity. This simulation showed that the wild-type AFP was able to form a close "fit" to the ice/water interface, employing a mixture of contacts from other polar groups and improved "steric matching" of the peptide shape to the ice/water interface. This conclusion was also reached by Lal et al. (1993) in docking studies: steric fit and polar group contacts were both found to be important. These findings may well be important in the design of synthetic antifreeze molecules.

The constraints of serial computation for the simulation of these systems were clearly visible, the major problems being the inability of the peptide to "roll" about its long axis during the short observation time that precluded a determination of the preferred orientation of the peptide at an ice/water interface. We are repeating the MD simulations with the peptide in other initial orientations and comparing the extent of binding to the ice. Problems associated with short observation times in the simulation will be addressed using parallel architectures. The lack of rolling reflects the low temperature, the high viscosity of the solution, and the sluggish kinetics (the diffusion coefficient of water molecules in the liquid was about five times smaller than bulk water at 300 K).

Acknowledgments

The authors are pleased to acknowledge the financial support of Unilever PLC and a matching grant from the Cornell Center for Advanced Technology in Biotechnology, which is sponsored by the New York State Science and Technology Foundation, a consortium of industries and the National Science Foundation. One of the authors (A.W.) acknowledges the support of the Cornell Materials Science Center for a Research Experience for Undergraduates fellowship provided by the National Science Foundation. The computer time on a Cray C-90 was provided by the Pittsburgh Supercomputer Center.

Literature Cited

Aqvist, J., P. Sandblom, T. A. Jones, M. E. Newcomer, W. F. van Gunsteren, and O. Tapia, "Molecular Dynamics Simulations of the Holo and Apo Forms of Retinol Binding Protein: Structural and Dynamical Changes Induced by Retinol Removal," *J. Mol. Biol.*, **192**, 593 (1986).

Barbato, G., M. Ikura, L. E. Kay, R. W. Pastor, and A. Bax, "Backbone Dynamics of Calmodulin Studied by N Relaxation Using Inverse Detected Two-Dimensional NMR Spectroscopy: The Central Helix Is Flexible," *Biochemistry*, **31**, 5269 (1992).

Berendsen, H. J. C., J. P. M. Postma, W. F. van Gunsteren, and J. Hermans, "Interaction Models for Water in Relation to Protein Hydration," *Intermolecular Forces*, Reidel, New York, pp. 331–342 (1981).

Brooks, B. R., R. E. Bruccoleri, B. D. Olafson, D. J. States, S. Swaminathan, and M. Karplus, "CHARMM: A Program for Macromolecular Energy, Minimization, and Dynamical Calculations," *J. Comp. Chem.*, **4**, 187 (1983).

Chakrabartty, A., V. S. Ananthanaraynan, and C. L. Hew, "Structure-Function Relationships in a Winter Flounder Antifreeze Polypeptide: I. Stabilization of an α-Helical Antifreeze Polypeptide by Charged-Group and Hydrophobic Interactions," *J. Biol. Chem.*, **264**, 11307 (1989a).

Chakrabartty, A., D. S. C. Yang, and C. L. Hew, "Structure-Function Relationship in a Winter Flounder Antifreeze Polypeptide: III. Alteration of the Component Growth Rates of Ice by Synthetic Antifreeze Polypeptides," *J. Biol. Chem.*, **264**, 11313 (1989b).

Chou, K., "Energy-Optimized Structure of Antifreeze Protein and its Binding Mechanism," *J. Mol. Biol.*, **223**, 509 (1992).

Cook, S. J., and P. Clancy, "Impurity Segregation in $A/A_{1-x}B_x$ Heterostructures during Liquid Phase Epitaxy," *J. Phys. Chem.*, **99**, 2175 (1993).

Davies, P. L., A. H. Roach, and C. L. Hew, "DNA Sequence Coding for an Antifreeze Protein Precursor from Winter Flounder," *Proc. Nat. Acad. Sci. U. S. A.*, **79**, 335 (1982).

Deutsch, P. W., B. N. Hale, R. C. Ward, and D. A. Reago, Jr., "Structural Studies of Low Temperature Ice I_h Using a Central Force Potential Model," *J. Chem. Phys.*, **78**, 5103 (1983a).

Deutsch, P. W., B. N. Hale, R. C. Ward, and D. A. Reago, Jr., "Theoretical Studies of the Structure of a Model Bulk Ice I_h near 300 K Using a Central Force Potential Model," *J. Phys. Chem.*, **87**, 4309 (1983b).

Eastman, J. T., and A. L. DeVries, "Antarctic Fishes," *Sci. Amer.*, **101**, 106 (1980).

Feeney, R. E., T. S. Burcham, and Y. Yeh, "Antifreeze Glycoproteins from Polar Fish Blood," *Ann. Rev. Biophys. Biophys. Chem.*, **15**, 59 (1986).

Fourney, R. M., S. B. Joshi, K. H. Ming, and C. L. Hew, "Heterogeneity of Antifreeze Polypeptides From the Newfoundland Winter Flounder Pseudopleuronectes Americanus," *Can. J. Zool.*, **62**, 28 (1984).

Grinnell, F., and M. K. Feld, "Fibronectin Adsorption on Hydrophilic and Hydrophobic Surfaces Detected by Antibody Binding and Analyzed during Cell Adhesion in Serum-containing Medium," *J. Biol. Chem.*, **257**, 4888 (1982).

Han, K., and B. N. Hale, "Monte Carlo Study of a Simple Model Bulk-Ice-Ih System: P-T Melting Behavior at Constant Volume," *Phys. Rev. B*, **45**, 29 (1992).

Hew, C. L., and G. L. Fletcher, *Circulation, Respiration, and Metabolism*, Springer-Verlag, Berlin, pp. 553–563 (1985).

Horbett, T. A., "Adsorption of Proteins from Plasma to a Series of Hydrophilic-Hydrophobic Copolymers: II. Compositional Analysis with the Prelabeled Protein Technique," *J. Biomed. Mater. Res.*, **15**, 673 (1981).

Karim, O. A., P. A. Kay, and A. D. J. Haymet, "The Ice/Water Interface: A Molecular Dynamics Simulation Using the Simple Point Charge Model," *J. Chem. Phys.*, **92**, 4634 (1990).

Karim, O. A., and A. D. J. Haymet, "The Ice/Water Interface: A Molecular Dynamics Simulation Study," *J. Chem. Phys.*, **89**, 6889 (1988).

Knight, C. A., C. C. Cheng, and A. L. DeVries, "Adsorption of α-Helical Antifreeze Peptides on Specific Ice Crystal Surface Planes," *Biophys. J.*, **59**, 409 (1991).

Lal, M., A. H. Clark, A. Lips, J. N. Ruddock, and D. N. J. White, "Inhibition of Ice Crystal Growth by Preferential Peptide Adsorption: A Molecular Modelling Study," *Farad. Discuss.*, **95**, 299 (1993).

Lu, D. R., and K. Park, "Effect of Surface Hydrophobicity on the Conformational Changes of Adsorbed Fibrinogen," *J. Coll. Interf. Sci.*, **144**, 271 (1991).

Madura, J. D., A. Wierzbicki, J. P. Harrington, R. H. Maughon, J. A. Raymond, and C. S. Sikes, "Interactions of the D- and L-Forms of Winter Flounder Antifreeze Peptide with the [201] Planes of Ice," *J. Amer. Chem. Soc.*, **116**, 417 (1994).

McDonald, S. M., J. W. Brady, and P. Clancy, "Molecular Dynamics Simulations of a Winter Flounder Antifreeze Polypeptide in Aqueous Solution," *Biopolymers*, **33**, 1481 (1993).
McDonald, S. M., A. C. White, J. W. Brady, and P. Clancy, unpublished results (1994).
McDonald, S. M., "Molecular Modeling Studies of the Structure and Function of a Winter Flounder Antifreeze Polypeptide," PhD Thesis, Cornell Univ., Ithaca, NY (Jan., 1995).
Molecular Simulations, QUANTA Modeling Software, Release 3.4, Molecular Simulations, Inc., Waltham, MA (1992).
Pickett, M. H., G. Scott, P. Davies, N. Wang, S. Joshi, and C. Hew, "Sequence of an Antifreeze Protein Precursor," *Eur. J. Biochem.*, **143**, 35 (1984).
Pitt, W. G., K. Park, and S. L. Cooper, "Sequential Protein Adsorption and Thrombus Deposition on Polymeric Biomaterials," *J. Coll. Inter. Sci.*, **111**, 343 (1986).
Rao, U., M. M. Teeter, S. Erikson-Vitanen, and W. F. DeGrado, "Calmodulin Binding to α-Purothionin: Solution Binding and Modeling of the Complex," *Proteins: Struct., Funct., Genet.*, **14**, 127 (1992).
Scott, G. K., P. L. Davies, M. A. Shears, and G. L. Fletcher, "Structural Variations in the Alanine-Rich Antifreeze Polypeptides of Pleuronectinae," *Eur. J. Biochem.*, **168**, 629 (1987).
Stickle, D. F., L. G. Presta, K. A. Dill, and G. D. Rose, "Hydrogen Bonding in Globular Proteins," *J. Mol. Biol.*, **226**, 1143 (1992).
Van Gunsteren, W. F., and H. J. C. Berendsen, "Algorithms for Macromolecular Dynamics and Constraint Dynamics," *Mol. Phys.*, **34**, 1311 (1977).
Ward, R. C., J. M. Holdman, and B. N. Hale, "Monte Carlo Studies of Water Monolayer Clusters on Substrates: Hexagonal AgI," *J. Chem. Phys.*, **77**, 3198 (1982).
Weber, T. A., and F. H. Stillinger, "Molecular Dynamics Study of Ice Crystallite Melting," *J. Phys. Chem.*, **87**, 4277 (1983).
White, D. N. J., and C. Morrow, "Cyclic Tetrapeptides I: The Calculated Potential Energy Minima of Cyclic Tetrapeptides Composed of Small Amino-Acid Residues," *Comput. Chem.*, **3**, 33 (1979).
Yang, D. S. C., M. Sax, A. Chakrabartty, and C. L. Hew, "Crystal Structure of an Antifreeze Polypeptide and Its Mechanistic Implications," *Nature*, **333**, 232 (1988).

Manuscript received May 12, 1994, and revision received Oct. 11, 1994.